INTERNATIONAL JOURNAL FOR NUMERICAL METHODS IN FLUIDS, VOL. 8, 617–641 (1988)

CURVATURE-COMPENSATED CONVECTIVE TRANSPORT: SMART, A NEW BOUNDEDNESS-PRESERVING TRANSPORT ALGORITHM

P. H. GASKELL AND A. K. C. LAU

Department of Mechanical Engineering, University of Leeds, Leeds LS2 9JT, U.K.

SUMMARY

The paper describes a new approach to approximating the convection term found in typical steady-state transport equations. A polynomial-based discretization scheme is constructed around a technique called 'curvature compensation'; the resultant curvature-compensated convective transport approximation is essentially third-order accurate in regions of the solution domain where the concept of order is meaningful. In addition, in linear scalar transport problems it preserves the boundedness of solutions. Sharp changes in gradient in the dependent variable are handled particularly well. But above all, the scheme, when used in conjunction with an ADI pentadiagonal solver, is easy to implement with relatively low computational cost, representing an effective algorithm for the simulation of multi-dimensional fluid flows. Two linear test problems, for the case of transport by pure convection, are employed in order to assess the merit of the method.

KEY WORDS Higher order Boundedness Convective transport Curvature Finite difference

1. INTRODUCTION

This paper proposes a new approach to approximating the convection term in typical multi-dimensional steady-state transport equations, so as to produce physically reasonable results, particularly in circumstances where standard methods fail. This approach, called curvature-compensated convective transport (CCCT), yields an algorithm which strictly preserves the boundedness (monotonicity) of a convected scalar transport variable. As a result, sharp changes in gradient are handled particularly well. The method requires no special knowledge about the solution and all internal grid points, spanning the computational domain of interest, are treated identically.

The general steady-state convection–diffusion equation, written in Cartesian–tensorial form, for a scalar ϕ, can be stated as

$$\frac{\partial(u_j\phi)}{\partial x_j}=\frac{\partial}{\partial x_j}\left(\mu\frac{\partial\phi}{\partial x_j}\right)+S \tag{1}$$

and can be approximated in finite difference form by either (a) directly performing a local Taylor series expansion of the derivatives, ignoring truncation terms of a certain order, or by (b) integrating over a macro control volume and replacing the face values and derivatives by approximations based on either Taylor series expansions or some form of interpolation. Ideally, the resulting finite difference expressions will be both conservative and transportive[1] and possess

0271–2091/88/060617–25$12.50

Received 26 February 1987
Revised 17 June 1987

certain desirable properties such as stability, accuracy and boundedness. For finite difference approximations, such features are reflected in the formally asymptotic truncation error terms. The importance of this error is evident in regions where the quantity

$$\left|\frac{\Delta x}{\phi}\frac{\partial \phi}{\partial x}\right| \sim O(1), \tag{2}$$

that is, in regions where high-wave-number Fourier components of ϕ are important to the solution[2]—such is the case in many problems of physical interest.

In parts of the solution domain where ϕ and u_j are smoothly varying functions, higher-order approximations such as the QUICK[3] (Quadratic Upstream Interpolation for Convective Kinematics) and CUI[4] (Cubic Upwind Interpolation) schemes (see also the cubic upwind scheme of Agarwal,[5] although it should be noted that this approximation is non-conservative) handle equation (1) quite adequately. However, in the presence of sharp changes in gradient or strong sources (sinks), relation (2) holds and the truncation error is of the same order of magnitude as the approximation. Consequently, short-wavelength errors quickly manifest themselves in such regions. The use of higher-order polynomial numerical approximations cannot resolve this problem, because the error terms, at all orders, are roughly of the same size as the function itself.

The CCCT finite difference approach described here overcomes these steep gradient problems by employing physically realistic constraints to ensure monotonic solutions while maintaining a high degree of accuracy. The method, based on a control volume formulation, is stable, conservative, transportive and essentially third-order accurate in regions where the concept of order is meaningful, but above all it is simple to implement. The implicit algorithm SMART, described later, generalizes quite conveniently for use in both two and three dimensions. Here we have chosen to perform a detailed investigation of two simple, yet severely demanding, linear two-dimensional steady-state test problems in order to demonstrate the general principles of CCCT and its potentials.

Section 2 gives an account of the philosophy which underpins CCCT, covering topics such as boundedness and convective stability, and a new convection boundedness criterion is presented in Section 3. This is then followed by a detailed derivation of the SMART algorithm in Section 4 and an outline of the solution strategy in Section 5. The test problems and associated results are discussed in Section 6, with particular attention being focused on the problem of pure convection. The overall performance of the approach is discussed and conclusions are given in Section 7.

2. ACCURACY, CONVECTIVE STABILITY AND BOUNDEDNESS

Accuracy

Classically, the accuracy of finite difference approximations is judged in terms of the leading truncation error term of a Taylor series expansion. This term is shown in Table I for five well known discretization schemes. However, the use of a Taylor series expansion to judge accuracy is only meaningful for those Fourier components of the real solution having a wave number $O(2\pi/L)$. For high wave numbers, $O(\pi/\Delta x)$, a formal increase in the order of accuracy will not improve the prediction, since the error is independent of the mesh size. It is the missing truncation terms (from any suitable numerical approximation) that would have a damping effect in these situations, restricting the propagation of such errors. The importance of this observation will become apparent later.

Table I. Some well known discretization schemes and their associated properties

Discretization scheme	Finite difference expression for $\phi_{i-1/2}$ when $u_{i-1/2}=u_0>0$	Leading truncation error term	Convective stability $\partial C_{IF}/\partial\phi_{i-1}$	Boundedness		Critical Peclet number	α
				Computed	Interpolative		
QUICK	$\frac{1}{8}(3\phi_i+6\phi_{i-1}-\phi_{i-2})$	$\frac{u_0\Delta x^3}{16}\phi'''_{i-1/2}$	$-\frac{3u_0}{8\Delta x}$(stable)	No	No	$\frac{8}{3}$	0
CUI	$\frac{1}{6}(2\phi_i+5\phi_{i-1}-\phi_{i-2})$	$\frac{u_0\Delta x^2}{24}\phi''_{i-1/2}$	$-\frac{u_0}{2\Delta x}$(stable)	No	No	3	$\frac{1}{24}$
Second-order upwind[13]	$\frac{1}{2}(3\phi_{i-1}-\phi_{i-2})$	$\frac{3u_0\Delta x^2}{8}\phi''_{i-1/2}$	$-\frac{3u_0}{2\Delta x}$(stable)	No	No	∞	$\frac{3}{8}$
Central differencing	$\frac{1}{2}(\phi_i+\phi_{i-1})$	$\frac{u_0\Delta x^2}{4}\phi''_{i-1/2}$	0 (neutral)	No	Yes	2	$-\frac{1}{8}$
Upwind	ϕ_{i-1}	$\frac{u_0\Delta x}{2}\phi'_{i-1/2}$	$-\frac{u_0}{\Delta x}$(stable)	Yes	Yes	∞	—

Convective stability

According to Leonard,[3] convective stability may be defined as the sensitivity of the convective influx, C_{IF}, into the control volume centered at $i-1$, of the nodal configuration shown in Figure 1, to the change in ϕ_{i-1}—namely $\partial C_{IF}/\partial\phi_{i-1}$. There are three possibilities:

$$\frac{\partial C_{IF}}{\partial \phi_{i-1}} \begin{cases} <0 & \text{stable sensitivity,} \\ =0 & \text{neutral sensitivity,} \\ >0 & \text{unstable sensitivity.} \end{cases} \tag{3}$$

In order to ensure convective stability, it is important to have a numerical negative feedback mechanism, such that any disturbance to ϕ_{i-1} from an outside influence will reduce or enhance C_{IF} in line with whether ϕ_{i-1} increases or decreases, respectively—ϕ_{i-1} will then converge to a value consistent with the numerical approximation.

From a purely physical viewpoint, convection is associated with the transport of fluid properties from upstream to downstream and, as such, any numerical approximation to convection should mirror this transportive feature. Hence it must possess an element of upwind bias, which, in relation to numerical models for convective transport, is an important concept. Alternatively, from a numerical standpoint, any numerical approximation to convection which is not upwind biased will lack convective stability and its associated coefficient matrix will be numerically unstable, and vice versa.[4]

It should be noted that the analogous property of diffusive stability, which depends upon the sensitivity of the diffusive influx, D_{IF}, into the control volume, to the change in ϕ_{i-1}, is always negative (for $\mu>0$) when the diffusive term is approximated by standard central differencing. This is sometimes enough to counterbalance the lack of convective stability. However, for flows in which the cell Peclet number is high (convection-dominated), it may be insufficient to avoid computational disaster.

Diagonal dominance and boundedness

Computational fluid dynamicists generally associate boundedness with the property of diagonal dominance, that is, the computed solution given by a numerical approximation is deemed to be bounded (devoid of unphysical overshoots or undershoots) if its associated coefficient matrix is diagonally dominant. If this condition holds, then the value of the dependent variable, at a desired grid point, represents simply a weighted average of its neighbours (in the absence of a source term in the governing equation). This guarantees that the solution is unconditionally bounded, with respect to the attendant boundary conditions, over the domain of interest. Also, the coefficient matrix is numerically stable.

The concept of diagonal dominance is useful in quantifying absolute boundedness (and similarly the numerical stability of the coefficient matrix) for a particular discretization scheme, but does not

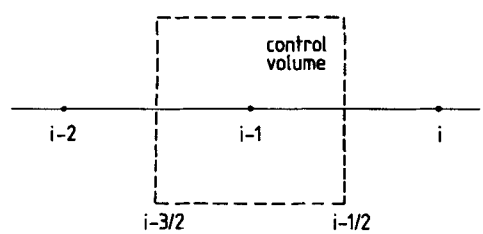

Figure 1. Nodal configuration showing a typical control volume

itself lead one to a deeper understanding of the underlying physics of the problem and may even result in misconceptions. For example, it is frequently stated that a discretization scheme may produce solutions with 'wiggles' when the cell Peclet number is greater than some critical value—see Table I. If this is exceeded, the coefficient matrix is no longer diagonally dominant. However, the cell Peclet number itself is not the cause of wiggles; its role is merely to exaggerate or diminish (depending on its relative magnitude) any undershoots or overshoots generated by the convection approximation being employed.

Both of the higher-order schemes, QUICK and CUI, mentioned earlier (unlike the simple upwind scheme) are, by virtue of the above definition, classified as being unbounded. Yet, if the conditions are favourable, they generate perfectly acceptable results. It is arguable, therefore, that strict adherence to diagonal dominance and its satisfaction as a prerequisite for bounded solutions could be misleading, since it represents, in some cases, only a sufficient condition for guaranteeing bouundedness. The question, therefore, that begs to be answered is—in the quest for higher-order, bounded, numerical models for convective transport, should computational fluid dynamicists focus their attention on ensuring that the associated coefficient matrix is diagonally dominant or should they look to satisfy another, more physically relevant, set of criteria? Here, the authors have chosen to pursue the latter alternative.

Normalization

In order to simplify the discussion of boundedness and for many other purposes, it is instructive and indeed useful to introduce a normalized dependent variable $\hat{\phi}_k$. Consider, without loss of generality, the right-hand face of the control volume centred at $i-1$ (as depicted in Figure 1). Here and in the ensuing analysis it will be assumed, for the sake of simplicity, that $u_{i-1/2}>0$.

$$\hat{\phi}_k=\frac{\phi_k-\phi_{i-2}}{\phi_i-\phi_{i-2}}, \tag{4}$$

with $k=i-2,\ i-3/2,\ \ldots,\ i$.

It is clear from (4) that the normalization employed is upwind biased. Also, as pointed out by Leonard[6] and as will become apparent later, $\hat{\phi}_{i-1}$ indicates the degree of upwind bias inherent in any normalized finite difference approximation to the face value $\phi_{i-1/2}$. For the case of one-dimensional flow and constant velocity u_0, the normalized integral form of equation (1), over this control volume, can be written as

$$\hat{\phi}_{i-1/2}-\hat{\phi}_{i-3/2}=\frac{\phi_{i-1/2}-\phi_{i-3/2}}{\phi_i-\phi_{i-2}}=\overline{S^*}, \tag{5}$$

where $\overline{S^*}$ is the net effective normalized source term, comprised of diffusion and physical source terms:

$$\overline{S^*}=\frac{\left[\left(\mu\frac{\partial\phi}{\partial x}\right)_{i-1/2}-\left(\mu\frac{\partial\phi}{dx}\right)_{i-3/2}\right]+\int_{i-3/2}^{i-1/2}S\,dx}{u_0(\phi_i-\phi_{1-2})} \tag{6}$$

In multi-dimensional flow problems, equation (5) is also valid, with additional contributions to $\overline{S^*}$ coming from the components of diffusion and convection in the associated mutually orthogonal directions. Hence equation (5) is a general representation for the transport of ϕ in the case of constant velocity.

A new perspective on boundedness constraints

Quadratic profiles, which one would expect to exist, relating $\hat{\phi}$ to x when $\hat{\phi}_{i-1} \approx 1$ or 0, are shown in Figure 2. A professional draftsman would, more than likely, draw the same profiles if asked to fit a curve through the three identical points (0, 0), (Δx, $\hat{\phi}_{i-1}$) and ($2\Delta x$, 1). A professional computational fluid dynamicist, on the other hand, would instinctively view this as a totally unreasonable representation of the physics (unless, that is, a large source term were known to be present in the system). Monotonic profiles similar to the ones shown would be considered to be much more representative and realistic; in which case the value of $\hat{\phi}_{i-1/2}$ lies between, or is locally bounded by, $\hat{\phi}_{i-1}$ and either 1 or 0, with the greatest variation in $\hat{\phi}$ taking place over a thin layer located upstream ($x \approx 0$) or downstream ($x \approx 2\Delta x$), respectively. The inherent violation of boundedness through using a quadratic profile is obvious. When $\hat{\phi}_{i-1} \approx 1$, $\hat{\phi}_{i-1/2}$ is too large ($\approx 9/8$) and the value of ϕ_i must increase (overshoot), enhancing the convective flux at $i+1/2$, in order to balance the high (unphysical) influx to the control volume centred at i. This lack of 'interpolative boundedness' (that is, the approximate face value $\phi_{i-1/2}$, lies outside the bounds of its neighbouring values at the nodes i and $i-1$) is also inherent in other high-order approximations, such as CUI and second-order upwinding. In order to satisfy interpolative boundedness, one requires that $\hat{\phi}_{i-1/2} \in (\hat{\phi}_{i-1}, 1]$ when $\hat{\phi}_{i-1} \in (-\infty, 1]$, and $\hat{\phi}_{i-1/2} \in [1, \hat{\phi}_{i-1})$ when $\hat{\phi}_{i-1} \in [1, \infty)$. Only the simple upwind and central difference approximations satisfy this condition. Any discretization scheme violating it may give values for the convective fluxes which exceed those that are physically possible. However, guaranteeing interpolative boundedness does not necessarily result in 'computed boundedness' (or 'computed monotonicity' within the monotonic range of $\hat{\phi}_{i-1}$). Computed boundedness is what one desires; that is, the computed solution should not

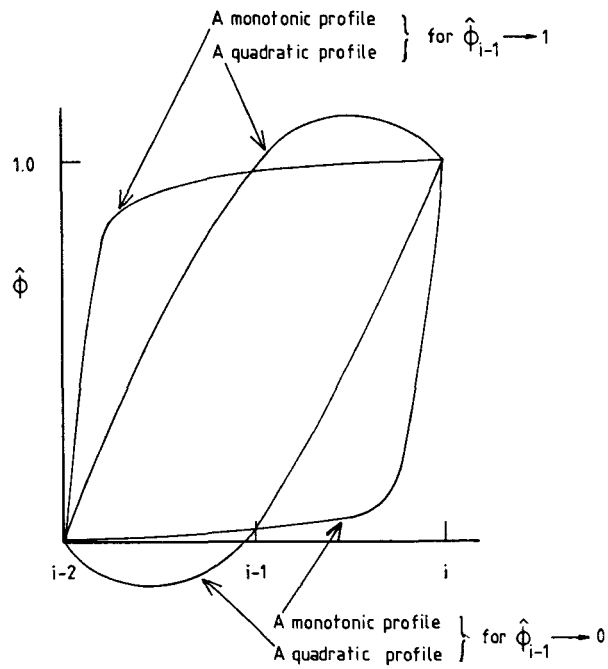

Figure 2. A schematic illustration of quadratic and monotonic profiles passing through the points (0, 0), (Δx, $\hat{\phi}_{i-1}$) and ($2\Delta x$, 1) in regions of potential undershoot and overshoot

contain any unphysical overshoots or undershoots and should remain bounded with respect to the attendant boundary values in the absence of a physical source term. In order to achieve computed boundedness, interpolative boundedness is a necessary (as explained earlier) but not sufficient condition.

If the normalized effective source term $\overline{S^*}$ in equation (5) is positive, physical considerations lead one to the conclusion that $\hat{\phi}_{i-1}$ must be greater than 0, and vice versa. In physical terms, if $\hat{\phi}_{i-1} \approx 0$, the face value $\phi_{i-1/2}$ must be dominated by the upstream conditions and $\overline{S^*}$ is negligibly small; while, if $\hat{\phi}_{i-1} \approx 1$, the downstream conditions prevail. In both situations a rapid change in ϕ occurs in a region considerably less than the local mesh spacing Δx and as a consequence there is no means by which it can be resolved numerically. For moderate gradients of ϕ, $\hat{\phi}_{i-1} \approx 0{\cdot}5$. Figures 3(a)–(c) show all possible variations of ϕ across three successive grid points in physical space for different $\hat{\phi}_{i-1}$ scenarios. For the computed solution to mimic the physical features shown in Figures 3(a)–(c), we must have

$$1 < \hat{\phi}_{i-1/2} \leqslant \hat{\phi}_{i-1}, \quad 0 \leqslant \hat{\phi}_{i-3/2} < \hat{\phi}_{i-1/2} \qquad \text{for} \quad \overline{S^*} > 0, \quad \hat{\phi}_{i-1} > 1, \tag{7a}$$

$$0 \leqslant \hat{\phi}_{i-3/2} \leqslant \hat{\phi}_{i-1} < \hat{\phi}_{i-1/2} \leqslant 1 \qquad \text{for} \quad \overline{S^*} \geqslant 0, \quad 0 \leqslant \hat{\phi}_{i-1} \leqslant 1, \tag{7b}$$

$$\hat{\phi}_{i-1} \leqslant \hat{\phi}_{i-1/2} < \hat{\phi}_{i-3/2} < 0 \qquad \text{for} \quad \overline{S^*} < 0, \quad \hat{\phi}_{i-1} < 0. \tag{7c}$$

It is not difficult to see that these three constraints (which are consistent with equation (5) and physical expectations) are both necessary and sufficient to ensure computed boundedness (independent of the number of nodal points involved in approximating the face value). Figure 3(d) shows an unrealistic profile for $\hat{\phi}$, in which, although $\overline{S^*} > 0$ ($\hat{\phi}_{i-1/2} > \hat{\phi}_{i-3/2}$) within the control volume centred at $i-1$, the value of $\hat{\phi}_{i-1}$ is negative.

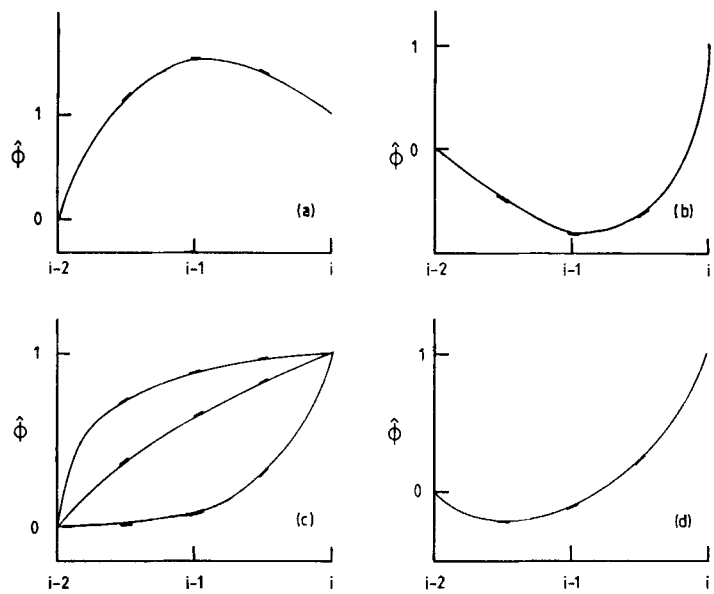

Figure 3. Profiles of $\hat{\phi}$ across three successive grid points, indicating physically realistic scenarios: (a) $\hat{\phi}_{i-1} > 1$ (cf. inequality (7a)); (b) $\hat{\phi}_{i-1} < 0$ (cf. inequaltiy (7c)); (c) $\hat{\phi}_{i-1} \in [0, 1]$ (cf. inequality (7b)); (d) $\hat{\phi}_{i-1} < 0$, $\overline{S^*} > 0$, $\hat{\phi}_{i-1/2} > \hat{\phi}_{i-3/2}$ (a physically unrealistic case)

3. A CONVECTION BOUNDEDNESS CRITERION

Unlike the QUICK scheme with its tantalising offer of superior accuracy and an end to the plagues of numerical diffusion, the ramifications of Leonard's conjectured monotonicity criterion[6] have remained more or less unnoticed by the computational fluid dynamics community at large. The underlying concepts are simple, having been fully verified and discussed in Section 2, and his rather loosely stated criterion can be generalized to give a more formally rigorous convection boundedness criterion (CBC) for implicit steady-state flow calculations.

Criterion. Define a continuous increasing function or union of piecewise continuous increasing functions f relating the modelled normalized face value $\hat{\phi}_{i-1/2}$, to the normalized upstream nodal value $\hat{\phi}_{i-1}$, that is, $\hat{\phi}_{i-1/2}=f(\hat{\phi}_{i-1})$. Then a finite difference approximation to $\phi_{i-1/2}$ is bounded if:

(i) for $\hat{\phi}_{i-1}\in[0, 1]$, f is bounded below by the function $\hat{\phi}_{i-1/2}=\hat{\phi}_{i-1}$ and above by unity and passes through the points (0, 0) and (1, 1);
(ii) for $\hat{\phi}_{i-1}\notin[0, 1]$, f is equal to $\hat{\phi}_{i-1}$.

This criterion is illustrated diagramatically in Figure 4.

The first condition ensures that the computed solution remains monotonic and satisfies the inequalities given in (7b), while the second relates to non-monotonic profiles and satisfies the inequalities given in (7a) and (7c).

The CBC is a necessary and sufficient condition for achieving computed boundedness if only three, neighbouring, upstream nodal values are used to approximate face values. Firstly, the approximated face value $\hat{\phi}_{i-1/2}$, satisfies interpolative boundedness for all values of $\hat{\phi}_{i-1}$ (this also applies to all other face values); hence no unrealistic convective fluxes can exist throughout the entire solution domain. Secondly, although the approximation to $\hat{\phi}_{i-1/2}$ is independent of $\hat{\phi}_{i-3/2}$

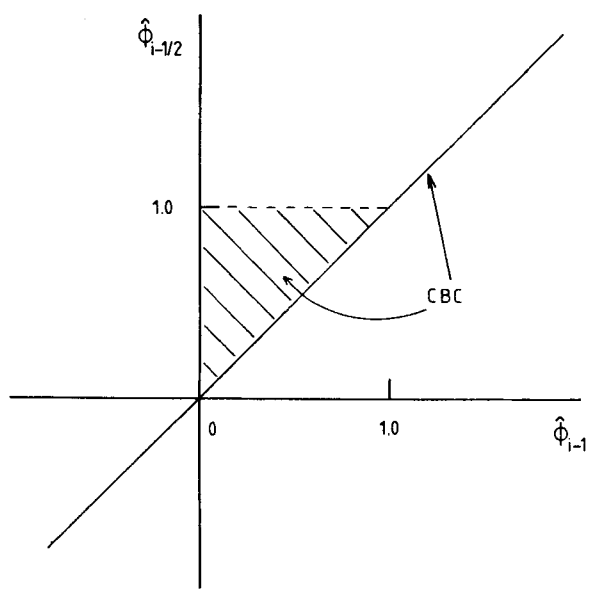

Figure 4. Diagrammatic representation of the convection boundedness criterion plotted in the $(\hat{\phi}_{i-1}, \hat{\phi}_{i-1/2})$ plane. The line $\hat{\phi}_{i-1/2}=\hat{\phi}_{i-1}$ and the shaded area indicate the region over which the criterion is valid

and $\overline{S^*}$, the CBC guarantees that, if S^* is positive $\hat{\phi}_{i-1} > 0$, and vice versa. This can be verified as follows:

(i) Along the line $\hat{\phi}_{i-1/2} = \hat{\phi}_{i-1}$, in the third quadrant (Figure 4), $\overline{S^*}$ must be less than or equal to zero because $\hat{\phi}_{i-3/2}$ is bounded between zero and $\hat{\phi}_{i-1}$; if f lies below this line, interpolative boundedness is violated; if f lies above this line, $\hat{\phi}_{i-3/2}$ may be lower than $\hat{\phi}_{i-1/2}$—if this happens, then undershoots may occur for $\overline{S^*} > 0$, as depicted in Figure 3(d), or a minimum might be exaggerated because $\hat{\phi}_{i-1}$ must decrease until $\hat{\phi}_{i-1/2} < \hat{\phi}_{i-3/2}$, in order to satisfy equation (5).

(ii) Along the line $\hat{\phi}_{i-1/2} = \hat{\phi}_{i-1}$, in the first quadrant, for $\hat{\phi}_{i-1} > 1$, $\overline{S^*}$ must be positive because $\hat{\phi}_{i-3/2}$ is below $\hat{\phi}_{i-1}$, if f lies above this line, interpolative boundedness is violated; if f lies below this line, $\hat{\phi}_{i-3/2}$ might be greater than $\hat{\phi}_{i-1/2}$ and hence, following a similar argument to that above, overshoots or the exaggeration of a maximum may occur.

(iii) If f lies within the shaded area (the monotonic range, shown in Figure 4), $\overline{S^*}$ must be positive because $\hat{\phi}_{i-1/2}$ is always greater than $\hat{\phi}_{i-3/2}$. Finally, f must pass through the points (0, 0) and (1, 1) in order to satisfy the requirement that the solution should follow the line $\hat{\phi}_{i-1/2} = \hat{\phi}_{i-1}$ outside the monotonic range of $\hat{\phi}_{i-1}$.

Although the above argument is based on a one-dimensional analysis, it is not difficult to show that the CBC is also a necessary and sufficient condition for guaranteeing computed boundedness in general multi-dimensional fluid flow simulations (see Appendix I).

Boundedness versus accuracy

If the solution of a problem is to remain bounded, then the approximation to $\phi_{i-1/2}$ must satisfy the above CBC. Outside the monotonic range of $\hat{\phi}_{i-1}$ and for $\hat{\phi}_{i-1} \to 1$ or 0, the CBC is extremely stringent, see Figure 4. Under these situations the true variation in ϕ cannot be resolved numerically, since the width of the thin layer over which rapid changes in ϕ occur is much less than the mesh spacing Δx. A numerical error is unavoidably introduced which cannot be eliminated simply by a formal increase in the order of accuracy of the numerical approximation to $\phi_{i-1/2}$. Similarly, a reduction in mesh size will not remove these types of error, although such action would minimize their occurrence within the solution domain. Indeed, it can be shown,[7] by taking account of a limited number of the truncated derivative terms in standard approximations such as QUICK, that the relative error is a constant (for each) independent of the mesh size. Therefore a suitable approximation to $\phi_{i-1/2}$ is one which minimizes error propagation while avoiding undershoots or overshoots.

In Figure 5 the normalized profiles of some well known discretization schemes are shown, all of which are at least second-order accurate—except, that is, the pure upwind approximation. However, it can be seen from this figure that the latter is the only one which can be classed as being unconditionally bounded in terms of the CBC. Unfortunately, there is a catch, in the form of excessive numerical diffusion; this is surely now recognized as too high a price to pay in order to guarantee solutions without undershoots or overshoots. Also, it can be seen that all of the higher-order approximations pass through the point (1/2, 3/4). Indeed, as pointed out by Leonard,[6] when $\hat{\phi}_{i-1} = 1/2$, the most reasonable and accurate approximation to $\hat{\phi}_{i-1/2}$ can be found via linear interpolation (that is, $\hat{\phi}_{i-1/2} = 3/4$) in the absence of any other additional information—the upwind approximation fails to satisfy this rather obvious condition.

It is evident from Table I and Figure 5 that none of the five schemes given therein can unconditionally and simultaneously achieve monotonicity, high accuracy and convective stability. In order to realize such a goal, the use of some form of non-linear scheme is unavoidable, that is,

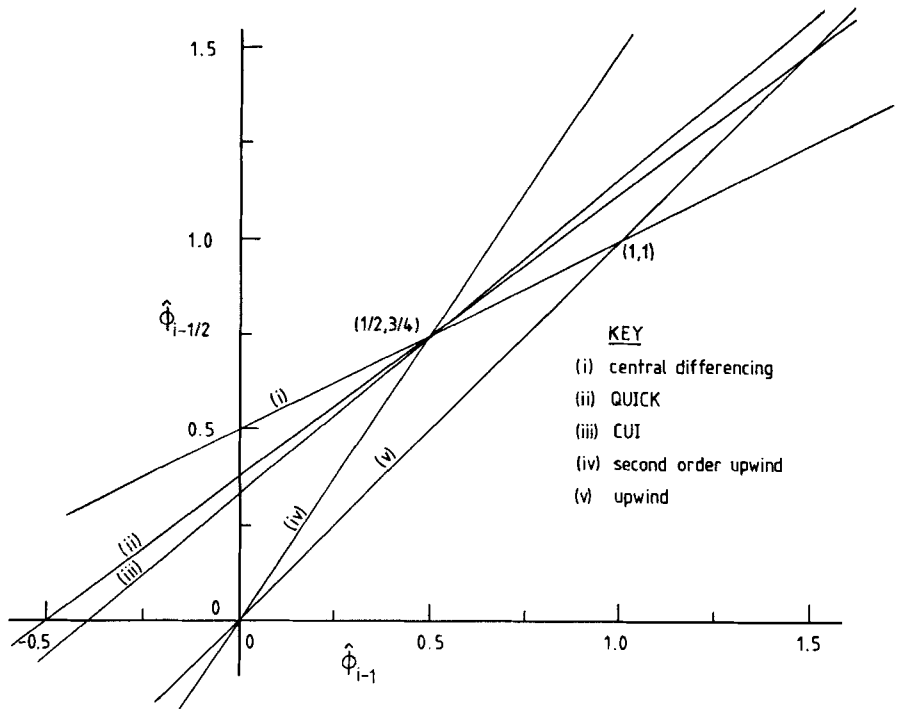

Figure 5. Normalized values of $\hat{\phi}_{i-1/2}$ for various well known approximations

$\hat{\phi}_{i-1/2}$ cannot be thought of as just a simple linear function of $\hat{\phi}_{i-1}$. The exponential interpolation function (EIF) proposed by Leonard,[6] which has the form $\phi_{i-1/2} = A + B\exp(Cx)$ (where A, B and C are uniquely determined by the value of the dependent variable at the nearest three upstream points), satisfies this requirement. This exponential approximation has shown itself to be well suited to explicit time-marching calculations for transient incompressible flow problems. Unfortunately, extension of the scheme to implicit steady-state flow calculations, particularly for the case of non-uniform mesh spacings, is not obvious. The boundedness/monotonicity-preserving approximation described in the next section is based on and satisfies the CBC and is referred to as curvature-compensated convective transport. It is quasi-linear rather than non-linear as in the case of Leonard's EIF.

4. CURVATURE-COMPENSATED CONVECTIVE TRANSPORT

An optimum upstream weighted approximation for convection

Although the order of accuracy of the various higher-order approximations to $\phi_{i-1/2}$, given in Table I range from $O(\Delta x^2)$ to $O(\Delta x^3)$, their predictive powers, in the absence of very steep gradients in the dependent variable ϕ, are comparable. Indeed, in relation to QUICK and CUI the authors have shown,[8] for a variety of laminar fluid flow problems, that the results achieved with both approximations are practically indistinguishable. This is not what one would expect if the order of accuracy of finite difference expressions is to be judged in relation to the largest of the truncation error terms, and is alien to established thinking. Interestingly enough, other authors[7] are known to

give credence and support to such findings. Therefore, on the basis of this paradox, it is postulated that any upwind biased approximation to $\phi_{i-1/2}$ which can be shown to contain, at most, a second-order truncation error should be capable of producing accurate solutions (in comparison with those obtained by pure upwinding).

Consider the right-hand face of the control volume centred at $i-1$ when $u_{i-1/2}>0$ and perform Taylor series expansions about the left and right nodes directly adjacent to it, giving

$$\begin{aligned}
\phi_i &= \phi_{i-1/2} + \frac{\Delta x}{2}\phi'_{i-1/2} + \frac{\Delta x^2}{8}\phi''_{i-1/2} + \frac{\Delta x^3}{48}\phi'''_{i-1/2} + \text{HOT},\\
\phi_{i-1} &= \phi_{i-1/2} - \frac{\Delta x}{2}\phi'_{i-1/2} + \frac{\Delta x^2}{8}\phi''_{i-1/2} - \frac{\Delta x^3}{48}\phi'''_{i-1/2} + \text{HOT},\\
\phi_{i-2} &= \phi_{i-1/2} - \frac{3\Delta x}{2}\phi'_{i-1/2} + \frac{9\Delta x^2}{8}\phi''_{i-1/2} - \frac{9\Delta x^3}{16}\phi'''_{i-1/2} + \text{HOT}.
\end{aligned} \tag{8}$$

By taking suitable combinations of the above expansions and ignoring the higher-order terms (HOT), it is not difficult to show that

$$\phi_{i-1/2} = \frac{6\phi_{i-1} + 3\phi_i - \phi_{i-2}}{8} - \frac{\Delta x^3}{16}\phi'''_{i-1/2}. \tag{9}$$

Similarly, it can be shown that a measure of the upstream curvature is given by

$$(\phi_i - 2\phi_{i-1} + \phi_{i-2}) = \Delta x^2 \phi''_{i-1/2} + \frac{\Delta x^3}{2}\phi'''_{i-1/2}. \tag{10}$$

We now introduce (10) into (9), in a rather novel way, to give

$$\begin{aligned}
\phi_{i-1/2} = {} & (\tfrac{3}{4} + 2\alpha^-)\phi_{i-1} + (\tfrac{3}{8} - \alpha^-)\phi_i - (\tfrac{1}{8} + \alpha^-)\phi_{i-2}\\
& + [\alpha^- \Delta x^2 \phi''_{i-1/2} - (\tfrac{1}{16} - \tfrac{1}{2}\alpha^-)\Delta x^3 \phi'''_{i-1/2} + \ldots],
\end{aligned} \tag{11}$$

where α^- (the $-$ denoting at the right-hand face of the control volume centred at $i-1$) is a variable parameter that remains to be determined. The leading truncation error term in (11) is $O(\alpha^- \Delta x^2)$ and by combining the above expressions this way we have effectively introduced a second-order curvature compensation in α^- to the third-order accurate approximation for $\phi_{i-1/2}$. An analogous expression for the left-hand face of the control volume can be derived in exactly the same way. Normalizing equation (11) according to (4) and ignoring the truncation error terms, we have that

$$\hat{\phi}_{i-1/2} = (\tfrac{3}{4} + 2\alpha^-)\hat{\phi}_{i-1} + (\tfrac{3}{8} + \alpha^-). \tag{12}$$

The approximation to the face value given by equation (11), or equation (12) in normalized form, can be viewed as an optimum upstream weighted approximation for convection because, by a suitable choice of α^- at each node, various discretization schemes are readily obtained, such as Leonard's EIF and QUICK approximation, CUI, second-order upwinding and central differencing. In a similar fashion, if α^- is fixed at a suitable constant value everywhere, several of these higher-order polynomial schemes can be formed—see Table I. However, since $\alpha^- = 0$ is indicative of the maximum accuracy obtainable, $O(\Delta x^3)$, it is essential to optimize this parameter in such a way that it lies as close to zero as possible, while preserving boundedness and ensuring that convective stability is maintained for all values of α^- throughout the solution domain.

Determination of the variable α^-

The value of $\hat{\phi}_{i-1/2}$ predicted when $\alpha^- = 0$ over the monotonic range of $\hat{\phi}_{i-1}$ is greater than 1 when $\hat{\phi}_{i-1} > 5/6$. Therefore the minimum requirement to keep ϕ bounded in this situation is to set $\hat{\phi}_{i-1/2} = 1$ for $\hat{\phi}_{i-1} \in (5/6, 1]$ (line cd in Figure 6). We have already seen that when $\alpha^- = 0$ and $\hat{\phi}_{i-1} \approx +0$, $\hat{\phi}_{i-1/2}$ is too large, causing an undershoot problem, and it is clear from Figures 4 and 5 that this poses a greater threat to boundedness. Also, it is obvious that if, as is the strategy here, the case $\alpha^- = 0$ is the preferred choice in terms of achieving maximum accuracy, there is the need for a further constraint on $\hat{\phi}_{i-1/2}$ in this region. It is possible for our professional computational fluid dynamicist to find such a constraint, if in addition to $\hat{\phi}_{i-1/2} \in (\hat{\phi}_{i-1}, 1]$ one insists that $\hat{\phi}_{i-1/2}$ is determined predominately by the two upstream values, $\hat{\phi}_{i-2}$ at $x = 0$ and $\hat{\phi}_{i-1}$ at $x = \Delta x$. This is a plausible assumption since the transport of ϕ by convection is only weakly dependent on the downstream conditions. When $\alpha^- = 0$ is used to approximate $\hat{\phi}_{i-1/2}$, the implied normalized upstream nodal value at $i - 3/2$ is zero when $\hat{\phi}_{i-1} = 1/6$ (a property of the quadratic profile). Within this potential undershoot region ($\hat{\phi}_{i-1} \approx +0$) boundedness can be preserved by imposing a linear relationship (line ab in Figure 6) between the point (1/6, 1/2) on the $\alpha^- = 0$ line and the origin. The choice of a straight line and the point (1/6, 1/2) is completely arbitrary, giving a much larger reduction in $\hat{\phi}_{i-1/2}$, compared with the $\alpha^- = 0$ line over the same region. Over the remainder of the monotonic range, $\hat{\phi}_{i-1} \in [1/6, 5/6]$, $\alpha^- = 0$. Therefore α^- is uniquely defined for $\hat{\phi}_{i-1} \in [0, 1]$, the CBC is satisfied and high accuracy, for moderate values of $\hat{\phi}_{i-1}$, is achieved.

Ideally, outside the monotonic range of $\hat{\phi}_{i-1}$, the two lines which deviate from the $\alpha^- = 0$ line should be joined with the latter in order to achieve 'high accuracy' (in terms of a Taylor series expansion). However, the line $\hat{\phi}_{i-1/2} = \hat{\phi}_{i-1}$ is the only possible choice if the CBC is to be satisfied. Here, there is a conflict between accuracy and boundedness—both cannot be achieved simultaneously. Further information is necessary to resolve this problem (for example, global optimization between $\hat{\phi}_{i-1/2}$ and $\hat{\phi}_{i-3/2}$, such that the inequalities (7a) and (7c) are satisfied, would

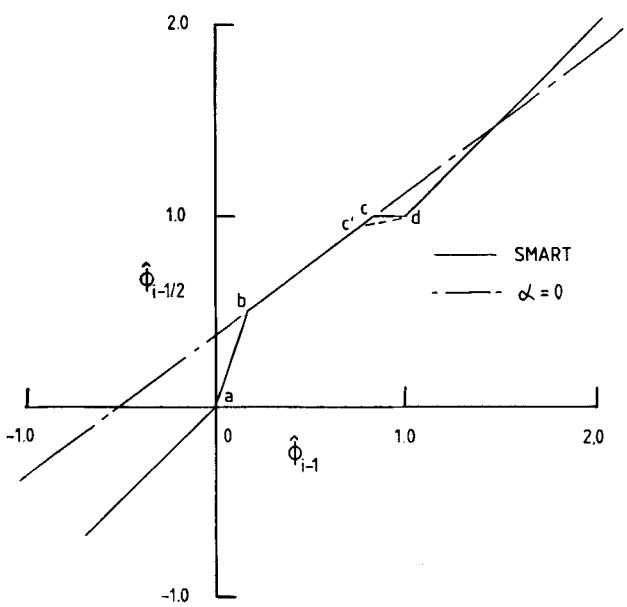

Figure 6. Representation of the SMART algorithm in the $(\hat{\phi}_{i-1}, \hat{\phi}_{i-1/2})$ plane

require the use of more than three nodal values to approximate the face value). However, the satisfaction of the boundedness constraint appears to be more important than the quest for accuracy—the latter being relegated to one of secondary importance in regions where high-wave-number components of ϕ dominate, as explained earlier. Therefore the line $\hat{\phi}_{i-1/2} = \hat{\phi}_{i-1}$ should be employed for $\hat{\phi}_{i-1} \notin [0, 1]$. It is important to note that the use of the line $\hat{\phi}_{i-1/2} = \hat{\phi}_{i-1}$, via equation (11), is a second-order, not first-order, approximation.

The SMART algorithm

The preceding analysis and the piecewise continuous function thus generated, which ensures bounded solutions, can be conveniently summarized into what we term a Sharp and Monotonic Algorithm for Realistic Transport (SMART) by convection. Its inherent simplicity is self-evident:

$$\alpha^- = \left[\frac{\hat{\phi}_{i-1/2} - \frac{3}{8}(2\hat{\phi}_{i-1} + 1)}{2\hat{\phi}_{i-1} - 1} \right], \tag{13}$$

where

$$\hat{\phi}_{i-1/2} = \begin{cases} \hat{\phi}_{i-1} \quad \text{and} \quad \alpha^- \in (-1/8, 3/8) & \text{if} \quad \hat{\phi}_{i-1} \notin [0, 1], \\ 3\hat{\phi}_{i-1} \quad \text{and} \quad \alpha^- \in (0, 3/8] & \text{if} \quad \hat{\phi}_{i-1} \in [0, 1/6), \\ 1 \quad \text{and} \quad \alpha^{-1} \in [-1/8, 0) & \text{if} \quad \hat{\phi}_{i-1} \in (5/6, 1], \\ \frac{3}{8}(2\hat{\phi}_{i-1} + 1) \quad \text{and} \quad \alpha^- = 0 & \text{if} \quad \hat{\phi}_{i-1} \in [1/6, 5/6]. \end{cases} \tag{14}$$

It is clear that $\hat{\phi}_{i-1}$ must be known before $\hat{\phi}_{i-1/2}$ or α^- can be determined. For implicit calculations this necessitates the use of an iterative process (even in the case of linear problems), that is, the use of previous known values of ϕ to calculate values for both $\hat{\phi}_{i-1}$ and $\hat{\phi}_{i-1/2}$, which in turn are used to determine α^- via (13). With these current values of α, spanning the solution domain, a new solution for ϕ can be obtained, the process being repeated until a converged solution is achieved. The functional dependence of α on $\hat{\phi}_{i-1}$ is shown in Figure 7.

All that remains is to show that equations (11)–(14) satisfy convective stability. Assuming constant velocity ($u = u_0$), we have that

$$\frac{\partial C_{\text{IF}}}{\partial \phi_{i-1}} = u_0 \frac{\partial(\phi_{i-3/2} - \phi_{i-1/2})}{\partial \phi_{i-1}} = u_0[-\tfrac{3}{8} - (\alpha^+ + 2\alpha^-)], \tag{15}$$

where α^+ is the corresponding value of the variable α at the left-hand face of the control volume centred at $i-1$. From the SMART algorithm we see that $\alpha \in [-1/8, 3/8]$ and in this range equation (15) is always less than zero—hence the convective stability property is satisfied. Note that α^- and α^+ can never be $-1/8$ simultaneously. The corresponding expression relating to $\phi_{i-3/2}$, when $u_{i-3/2} > 0$ follows quite naturally, as do those for $\phi_{i-1/2}$ when $u_{i-1/2} < 0$ and $\phi_{i-3/2}$ when $u_{i-3/2} < 0$, which can be found using an obvious reflection principle.

The effectiveness of the CCCT approach in modelling convection is demonstrated in Section 6 with the aid of two test problems in the limit as the diffusion and source terms in equation (1) tend to zero. A detailed investigation of the transport of step and box-shaped ϕ profiles by the process of pure convection is undertaken. Unlike the latter, the former test problem is not novel, having been adopted by a number of authors[7,9] for evaluating the relative performance of a variety of numerical approximations under the same conditions. Therefore, in order to avoid unnecessary repetition, and for the sake of clarity, only results obtained with the bounded, low-order, diffusive upwind and the unbounded high-order QUICK approximations are presented as a comparison with the SMART results. However, before proceeding with the comparisons, it is worthwhile dwelling on the important features of the solution strategy employed in the calculations.

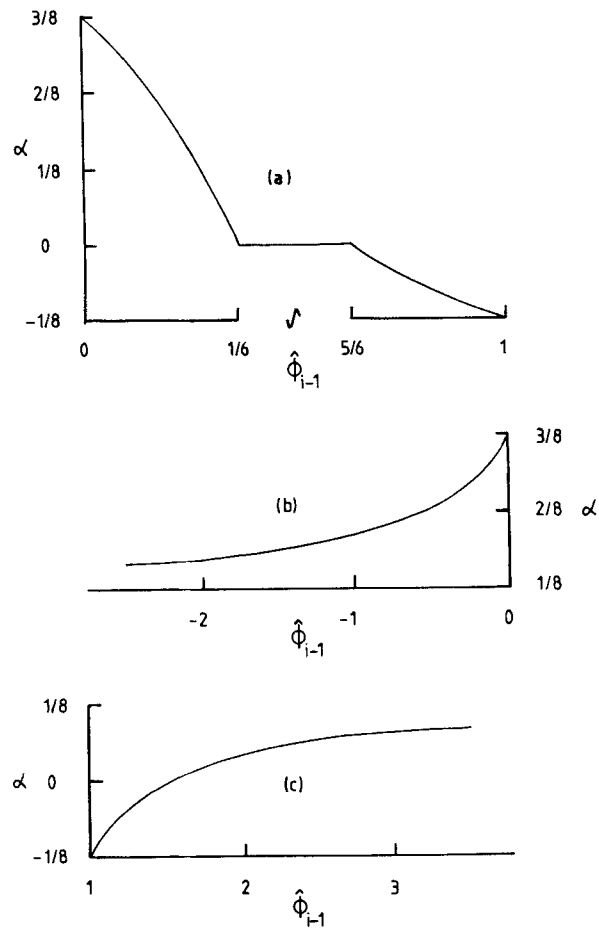

Figure 7. Functional dependence of α on $\hat{\phi}_{i-1}$ for the SMART algorithm: (a) $\hat{\phi}_{i-1} \in [0, 1]$; (b) $\hat{\phi}_{i-1} \in [-\infty, 0)$; (c) $\hat{\phi}_{i-1} \in (1, \infty]$

5. SOLUTION STRATEGY

Tridiagonal and pentadiagonal matrix algorithms (TDMA and PDMA) were used to solve the coefficient matrices generated by the upwind and QUICK/CCCT approximations, respectively, employing an alternating direction implicit (ADI) procedure. During the course of the present study it was found that the use of a PDMA (see Appendix II) rather than a TDMA solver, in respect of the higher-order approximations, was both cost effective and efficient. The cost relative to that for the upwind approximation solved with a TDMA was estimated to be of the order of 50% higher—the increase being attributed (mainly) to the prolonged assembly time of the coefficient matrix in the case of the higher-order schemes rather than being due to the solvers themselves (since the approximations were coded in a generally applicable form covering the possibility of non-uniform mesh spacing). Also, the use of a PDMA did not affect the stability or convergence of the solutions. These findings are in contrast to those reported in a recent study by Syed *et al.*[10] in similar circumstances.

The application of boundary conditions when higher-order approximations to convection are used can lead to complications. Therefore in the present study the first-order upwind approximation was applied at all boundaries in each case. This was done for the sake of simplicity and in the belief that, for the test problems under consideration, it would have only a very small effect on the overall accuracy of the results. The computational grids quoted for the test problems described in Section 6 are inclusive of internal and boundary nodes, the latter coinciding with the physical boundary of the solution domain.

The simultaneous use of the lines $\hat{\phi}_{i-1/2} = 1$ and $\hat{\phi}_{i-1/2} = \hat{\phi}_{i-1}$ for $\hat{\phi}_{i-1} \in (5/6, \infty)$, shown in Figure 6, may generate non-unique solutions in the absence of a source term in the governing equation for ϕ. The value of ϕ at the ith node in the discrete approximation is indeterminable (this may also depend on the starting conditions). On the other hand, if a source term is present the value of ϕ_i will be uniquely determined by the magnitude of the source term there. This problem is easily overcome by relaxing slightly the constraint at the point c in Figure 6. In obtaining the results of the next section the authors effected a 5% decrease in the value of $\hat{\phi}_{i-1/2}$ at this point, giving a new point c′ on the $\alpha = 0$ line. The choice of 5% is completely arbitrary but has been kept small in order that the new line joining d to c′ (shown exaggerated as a broken line) returns to the line $\alpha = 0$ quickly, for the reasons given earlier. This action gives a one-to-one relationship between $\hat{\phi}_{i-1/2}$ and $\hat{\phi}_{i-1}$, and a unique interlinking between the values of ϕ at all computational grid points. Note that the bounds on α and $\hat{\phi}_{i-1}$, in these regions must be modified accordingly in the SMART algorithm.

The relationship between $\hat{\phi}_{i-1/2}$ and $\hat{\phi}_{i-1}$ in the SMART algorithm is piecewise linear but their non-linear interaction via α over the different ranges of $\hat{\phi}_{i-1}$ represents a novel phenomenon in relation to implicit flow calculations, in that the scheme may appear to be capable of producing two 'non-stationary' solutions for the problem under consideration. This is a consequence of the direct dependence of the coefficients making up the coefficient matrix upon the dependent variable itself. For example, the two vectors $\boldsymbol{\phi}_1$ and $\boldsymbol{\phi}_2$ will be seen to be the solutions to a problem if their corresponding coefficient matrices are $\mathbf{A}_1(\boldsymbol{\phi}_2)$ and $\mathbf{A}_2(\boldsymbol{\phi}_1)$, respectively, such that

$$\mathbf{A}_1(\boldsymbol{\phi}_2)\boldsymbol{\phi}_1 = 0, \qquad \mathbf{A}_2(\boldsymbol{\phi}_1)\boldsymbol{\phi}_2 = 0 \tag{16}$$

(assuming no source term). Indeed the real solution vector $\boldsymbol{\phi}$ must satisfy

$$\mathbf{A}(\boldsymbol{\phi})\boldsymbol{\phi} = 0. \tag{17}$$

The simplest and most satisfactory way to overcome the problem of non-stationary solutions is to under-relax α by a factor r (a constant over the solution domain) when it is updated, in the following manner:

$$\alpha = \alpha^* + r(\alpha - \alpha^*), \tag{18}$$

where α^* represents the previous iterative value of α. In certain situations it may be necessary to experiment with the value of r before a stationary solution can be obtained. The authors have used the SMART algorithm for the simulation of a variety of complex turbulent fluid flow problems and have found the latter to be the exception rather than the rule. A value of 0·6 was found to be optimal for the test problems considered in Section 6.

The results presented in the next section conform to the following convergence criteria applied at all computational grid points:

$$\left| \frac{\phi^{n+1} - \phi^n}{\phi^n} \right| < 10^{-4}, \tag{19}$$

when n denotes the nth iterative cycle.

6. TEST PROBLEMS AND RESULTS

(i) Pure convection of a step profile

The flow configuration shown in Figure 8(a) constitutes a simple yet stringent test problem for examining the relative performance of different numerical approximations to convection because of the extremely sharp (indeed infinite) gradient in ϕ that exists. The cell Peclet number is of course infinite. A comparison of the numerical solutions obtained with upwind, QUICK and SMART along the vertical central plane of the solution domain on a 21×21 regular mesh is presented in Figures 8(b)–(d) for different flow angles θ. It can be seen that the upwind approximation results in a very diffuse ϕ profile for all three values of θ. This corruption of the steady-state solution is due solely to the influence of artificial (numerical) diffusion, which is seen to be the most severe at the maximum flow angle, $\theta = 45°$. On the other hand, the steep gradient is fairly well preserved by the QUICK approximation at all flow angles; unfortunately, each solution exhibits an oscillatory behaviour but, more seriously, sections of the resultant profiles are seen to lie outside the physical bounds of the solution domain $\phi \in [1, 2]$. However, despite these undesirable features, two points in particular should be noted. Firstly, the oscillations do not grow in strength but die out rather quickly—demonstrating that the leading truncation terms in the QUICK approximation have a strong stabilizing effect. Secondly, the magnitude of the undershoot is greater than that of the overshoot and the difference is more pronounced at the smaller flow angle ($\theta = 25°$).

In contrast to the above, both accuracy and boundedness is achieved by the SMART approximation. The sharp gradient in ϕ is again fairly well preserved by the SMART algorithm and the solution is free from spurious oscillations. Moréover, the results demonstrate that these rather desirable features are not very sensitive to the orientation of the flow field, that is, to the flow angle. This feature is important, particularly in relation to the simulation of complex recirculating fluid flows.

Computational cost.

Computational cost, or economy, is undoubtedly an important consideration when selecting a numerical approximation to perform a particular task. In relation to this test problem the total computational cost (sum of the central processing (CPU) time required for coefficient assembly, matrix inversion by TDMA or PDMA, etc.) was found to be roughly 1:13:18 for upwind:QUICK:SMART—based on the same computational mesh (all solutions satisfying the same convergence criterion). It must be emphasized that the increased cost in using either QUICK or SMART relative to that for the upwind approximation can be attributed (in the main) to the assembly of the matrix coefficients. However, rather than comparing computations performed on equal meshes to judge the relative costs of the different numerical approximations, it is instructive and arguably more meaningful to consider equal accuracy as a basis for determining economy. Accordingly, a measure of the relative accuracy ε for the above and other such problems can be defined as

$$\varepsilon = \frac{\sum_{\text{all nodes}} \left| \dfrac{\phi_{\text{exact}} - \phi_{\text{numerical}}}{\phi_{\text{exact}}} \right| \times 100\%}{N}, \tag{20}$$

where N is the number of computational grid points.

The flow angle $\theta = 45°$ was selected as a benchmark to examine the relative costs of the three approximations in achieving a solution whose accuracy (indicated by ε) is equal to a prescribed value $\varepsilon_{\min}$. Values of ε and corresponding CPU times are plotted (for successive grid refinement)

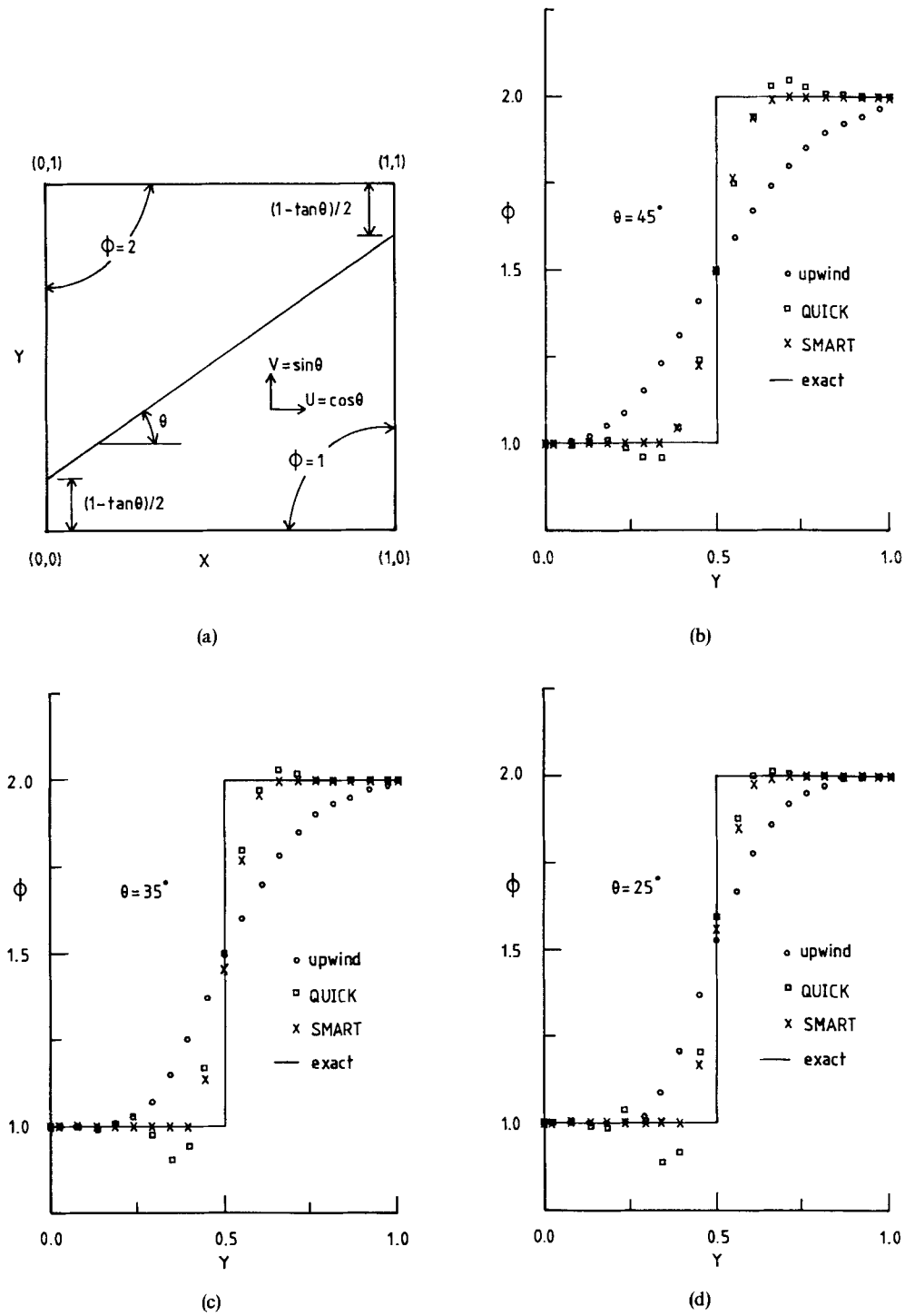

Figure 8. Pure convection of a step profile showing the flow configuration (a) and comparisons of the profile obtained using upwind, QUICK and SMART with that of the exact solution at different flow angles: (b) $\theta = 45°$; (c) $\theta = 35°$; (d) $\theta = 25°$

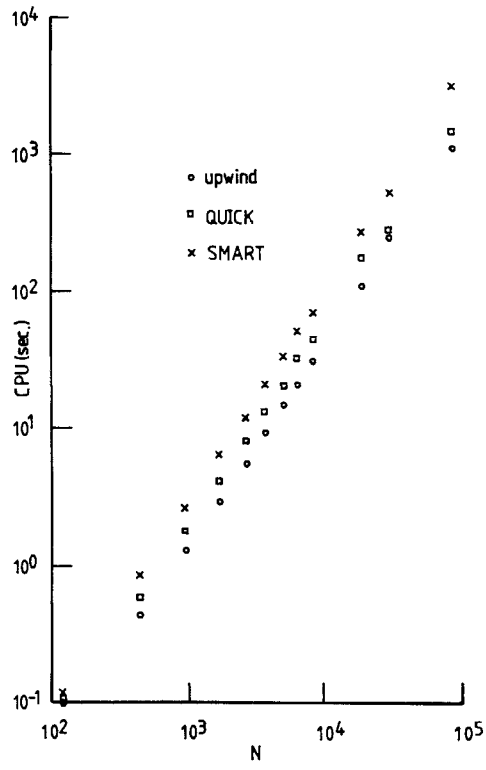

(a)

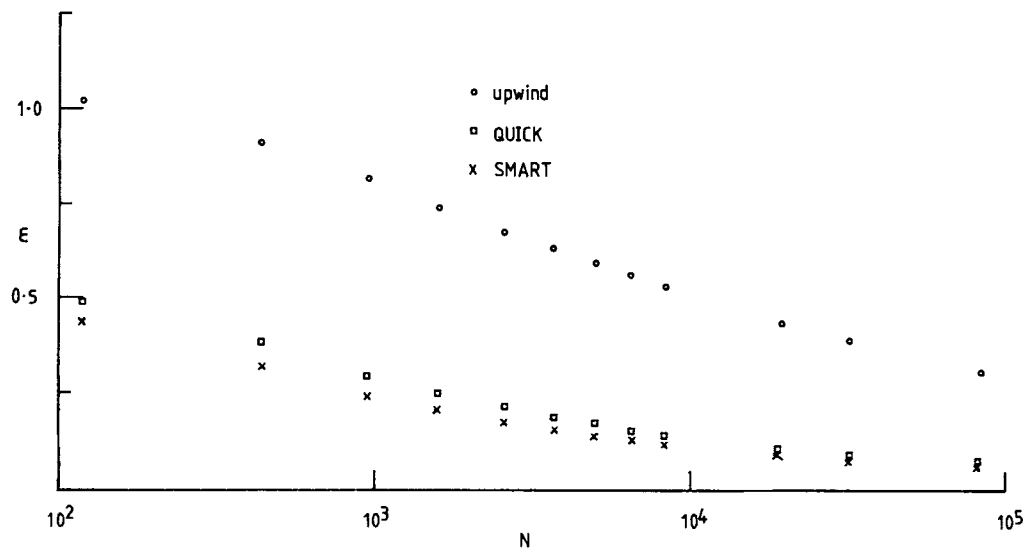

(b)

Figure 9. Comparisons of (a) the CPU time and (b) the relative error ε associated with the three approximations upwind, QUICK and SMART for different mesh densities

against N, in Figures 9(a) and (b), respectively. It can be seen that the relative costs (in CPU seconds) for $\varepsilon_{min} = 0{\cdot}3$ are approximately $1:1{\cdot}3:1{\cdot}3 \times 10^3$ for SMART:QUICK:upwind. Interestingly, the relative costs of using the SMART or QUICK approximation are comparable; that for the upwind approximation is certainly not and is, not surprisingly, extremely high. From Figures 8 and 9 it should also be noted that:

(i) All three solutions approach $\phi = \phi_d = 1{\cdot}5$ at the discontinuity, indicating the existence of an irreducible error that cannot be removed with successive grid refinement, which for the test problems considered here is roughly equal to

$$\left|\frac{\phi_{max} - \phi_d}{\phi_{min}}\right| \approx 0{\cdot}5.$$

(ii) Although the relative costs of the higher-order approximations are comparable, results obtained with QUICK will always contain overshoots or undershoots in the vicinity of very steep gradients, irrespective of successive grid refinement.

(iii) The span of N is very wide and the relaxation factors used in solving for the different approximations are undoubtedly important. In generating the data contained in Figure 9 no attempt was made to optimize convergence rates by selecting optimal relaxation factors for a particular approximation or mesh. These figures do, however, give a quantitative representation of the order of magnitude of the relative costs associated with the three approximations under investigation.

(iv) Exact solutions for real fluid flow problems can rarely be found, but nevertheless the present study does give a somewhat clearer indication of just how computationally expensive the upwind approximation can be in relation to achieving accurate converged solutions.

(ii) Pure convection of a box-shaped profile

Consider now the box-shaped ϕ profile shown in Figure 10(a) which is generated by imposing a step profile along the bottom and left-hand walls of the square solution domain. The value of ϕ is constant along a streamline. This test problem has been selected because the severe, rapid change in the gradient of ϕ is similar, in several ways, to many such profiles found in practical flow situations; for example, a severe peak profile characteristic of the change in turbulent kinetic energy across a thin shear layer.

As before, the numerically predicted profiles across the central vertical plane of the solution domain are compared. However, this time the results obtained with three different meshes, 21×21, 31×31 and 41×41, are presented (when $y^* = 0{\cdot}15$). Once again, the solutions obtained with the upwind approximation exhibit a highly dispersive pattern; Figures 10(b)–(d). The steep gradients in ϕ are almost completely smeared out by the numerical diffusion introduced there. Even when the grid is refined by a factor of two, the resultant solution represents only a minor improvement to that obtained on the coarser grid. The maximum predicted value of ϕ increases only marginally from 1·55 to 1·65 (as compared with the exact value of 2).

Figures 10(b)–(d) demonstrate quite clearly that both the QUICK and SMART approximations are able to resolve the sharp gradients on either side of the peaked profile. The latter, unlike the former, is free from any spurious oscillations and renders ϕ bounded over the solution domain. As with the first test problem, there are several points that should be noted:

(i) In real fluid flow calculations the insensitivity to grid refinement exhibited by the solutions obtained with the upwind approximation may give a false impression and lead one to believe that an accurate grid-independent solution has been reached.

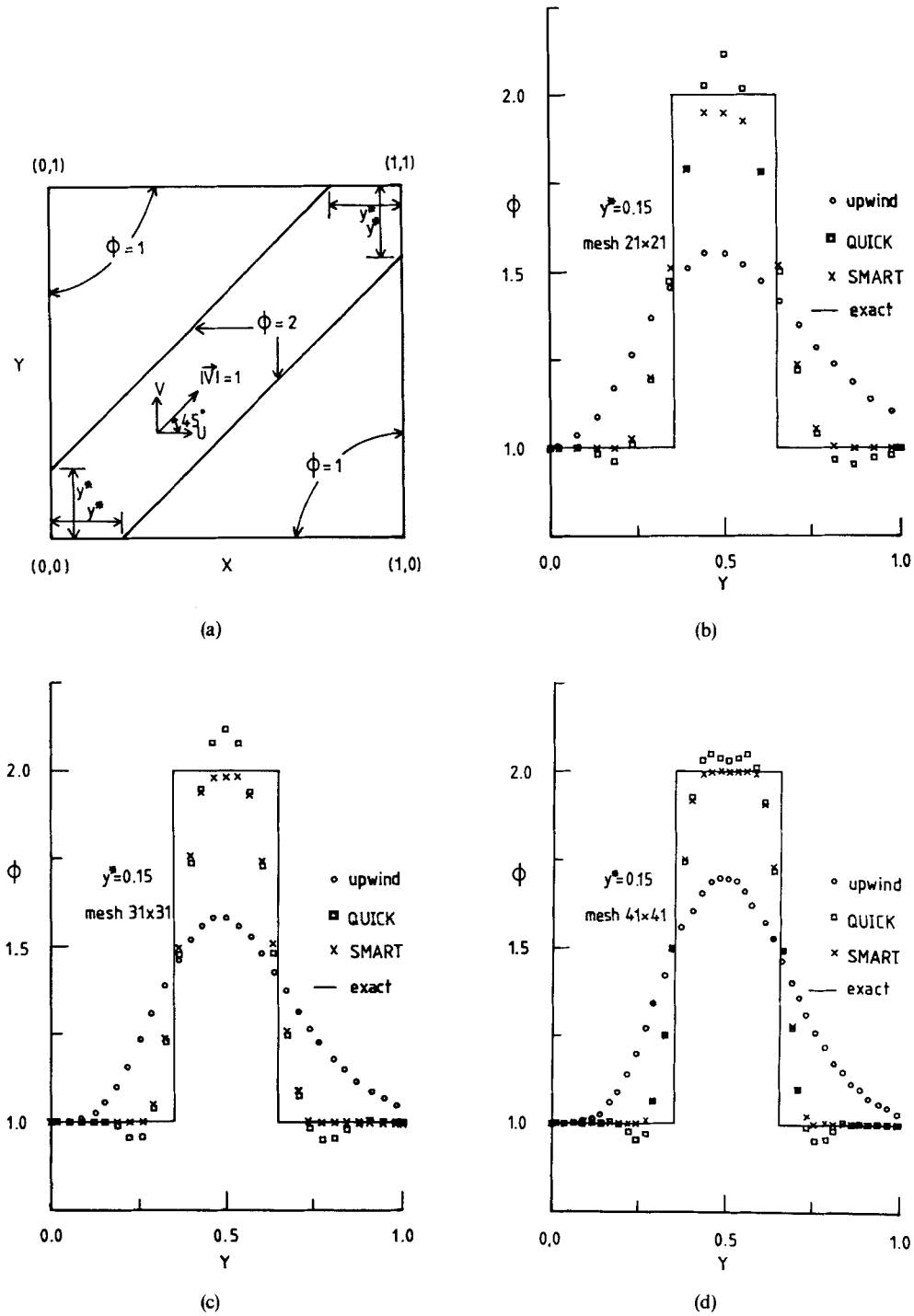

Figure 10. Pure convection of a box-shaped profile showing the flow configuration (a) and comparisons of the profiles obtained using upwind, QUICK and SMART with that of the exact solution for different mesh densities: (b) 21 × 21; (c) 31 × 31; (d) 41 × 41

(ii) Although the magnitude of the overshoot seen in the QUICK solution is substantially greater than that of its undershoots, the latter may lead to more serious problems in relation to real fluid flow simulations. For instance, if the turbulent kinetic energy or its dissipation rate were to become negative during a turbulent flow computation, the quality of the predicted solution would be greatly affected as a result of the strong coupling between these and the remaining mean flow quantities.

(iii) This test problem demonstrates quite well the ability of the SMART algorithm to preserve steep gradients without accentuating or creating any new maxima or minima.

7. CONCLUDING REMARKS

The present paper discusses boundedness constraints in relation to numerical models for convective transport. A convection boundedness criterion has been identified and rigorously validated. It represents a necessary and sufficient condition for computed boundedness (when the approximation to a face value is determined by, at most, three favourable upstream nodal values) and is valid for general multi-dimensional flow problems.

A curvature compensation methodology for use in conjunction with a control-volume-derived finite difference approximation to steady-state convection–diffusion transport equations has been presented. The primary goal of this paper has been to derive a new approach to approximating the convection term in equations of this type, called CCCT, such that the solution remains bounded and devoid of the potential to create spurious spatial oscillations in the vicinity of sharp changes in gradient in the dependent variable. The CCCT approximation possesses upwind bias and satisfies the requirements of convective stability.

The implicit CCCT algorithm SMART is applied to two test problems, one of which has been used by other authors in evaluating the relative performance of different numerical models for convection in terms of the degree of numerical diffusion associated with them. The second is somewhat different and exhibits a feature that is synonymous with real fluid flow problems. The SMART approximation is observed to perform extremely well, (a) exhibiting a relatively low level of anomalous spreading while also demonstrating its insensitivity to flow angle (unlike the low-order upwind approximation) and (b) resulting in fully bounded solutions that are free from spurious oscillations (unlike the high-order QUICK approximation).

Although it might be argued that the only true test of the virtues of such approximations lies in their applicability to the simulation of complex fluid flows, the experience gained in relation to the two test problems supports the following conclusions:

1. The SMART algorithm preserves boundedness and precludes the occurrence of spurious spatial oscillations (irrespective of the flow angle) while maintaining a high degree of accuracy. It is based on sound physical arguments and strict adherence to a convection boundedness criterion. Although the algorithm in its present form is the authors' preferred choice, there is no reason why others should not be derived which perform the same task, provided they satisfy the CBC stated in Section 3.
2. The SMART algorithm results in a relatively low level of numerical spreading, which is virtually insensitive to stream-to-grid obliqueness, and preserves steep gradients without accentuating or creating any new maxima or minima.
3. Although the CCCT approximation is non-linear, its implementation is extremely straightforward. Also, the computational cost associated with the use of this scheme is found to be relatively low.

4. Since each of the approximations listed in Table I can be found from equation (11) with α fixed at an appropriate constant value, the necessity of coding each one of them separately is alleviated. They can be replaced by just one approximation, even for the case of non-uniform mesh spacing.
5. The problem associated with the upwind scheme in relation to obtaining solutions of comparable accuracy to those found with the SMART and QUICK approximations on a much coarser mesh must question the wisdom of using low-order schemes in conjunction with a multi-grid convergence accelerator.

In view of these statements the authors believe that this work represents a significant contribution to the field of computational fluid dynamics: to quote Leonard[4]: 'Any method which simultaneously possess accuracy, stability algorithmic simplicity, and an easily comprehended physical interpretation would seem to be optimal'. CCCT certainly falls into this category and also includes a further essential ingredient—satisfaction of the boundedness property.

Note

The authors have employed the CCCT approximation to great effect in simulating several complex turbulent fluid flows for different geometries, some of the results of which can be found in a complementary publication.[11] Similarly, the method has been used in the solution of transient flow problems and is presently under investigation for use with a multi-gridding procedure.[12] These results and others will be appearing in due course.

ACKNOWLEDGEMENTS

The authors are grateful to British Gas plc for their continued financial support. Thanks are also due to T. David and N. G. Wright, of the Department of Mechanical Engineering, for their valuable comments in relation to this manuscript.

NOMENCLATURE

$\mathbf{A}$	coefficient matrix
L	length of solution domain
N	total number of nodes
r	relaxation factor
S	source term
$\overline{S^*}$	normalized effective source term
u_j	general velocity component
u_i	velocity at node i
x_j	general Cartesian co-ordinate
α	variable parameter in equation (8)
ϕ	scalar transport variable
μ	transport coefficient
θ	flow angle
Δx	mesh size in x-direction
U, V	horizontal and vertical velocity
X, Y	Cartesian co-ordinates
ε	relative error

Superscripts

$+/-$	value at left/right face of a control volume
$\hat{}$	a normalized value

Subscripts

i, $i-1$, etc. value at the nodes i, $i-1$, etc.

Other

$\tilde{}$	asymptotic limit
$O(\ )$	of the order of
$\in$	contained within
$\notin$	not contained within
$\delta \in [a, b)$	$a \leqslant \delta < b$, etc.

APPENDIX I: THE VALIDITY OF THE CBC IN MULTI-DIMENSIONS

Using a more convenient (but equally well known) notation to that employed in the main text, the general integral form for the transport of ϕ in the case of three-dimensional purely convective flow can be written as

$$\underset{x-\text{direction}}{[(\rho u\phi)_e-(\rho u\phi)_w]}+\underset{y-\text{direction}}{[(\rho v\phi)_n-(\rho v\phi)_s]}+\underset{z-\text{direction}}{[(\rho w\phi)_u-(\rho w\phi)_d]}=0, \tag{21}$$

where ρ and $\mathbf{u}(u, v, w)$ are the fluid density and velocities, respectively (both of which are not necessarily constant), and the subscripts e, w, n, etc. denote the average value of the quantity concerned, over that surface of the control volume centred at P, in that direction. The areas of each of the surfaces bounding the control volume are assumed to be equal and the components of $\mathbf{u}$ are taken to be positive in their corresponding co-ordinate directions.

For the case of pure convection, physical consideration leads one to the conclusion that ϕ must be bounded, over the whole solution domain, with respect to the attendant boundary conditions. In order for the computed solution to mirror this important feature, the computed ϕ_P must lie within the range of values of its nearest neighbours ϕ_E, ϕ_W, ϕ_N, ϕ_S, ϕ_U and ϕ_D. Therefore, in multi-dimensions, it is enough to prove that the CBC is both a necessary and sufficient condition for computed boundedness if it can be shown that the computed solution of ϕ_P (given, in each co-ordinate direction, by any approximation satisfying the CBC) cannot lie outside the range of values of its six neighbours. The proof is as follows.

If ϕ_P is assumed to lie outside the range ϕ_E to ϕ_W in the x-direction, ϕ_N to ϕ_S in the y-direction and ϕ_U to ϕ_D in the z-direction, then satisfaction of the CBC (in each direction) requires that $\phi_P = \phi_e$, $\phi_P = \phi_n$ and $\phi_P = \phi_u$ (it is important to note that this does not necessarily imply that the face values are replaced by a pure upwind approximation) and hence equation (21) can be written as

$$\phi_P=\frac{(\rho u\phi)_w+(\rho v\phi)_s+(\rho w\phi)_d}{(\rho u)_e+(\rho v)_n+(\rho w)_u} \tag{22}$$

and, by virtue of the continuity constraint,

$$(\rho u)_e+(\rho v)_n+(\rho w)_u=(\rho u)_w+(\rho v)_s+(\rho w)_d. \tag{23}$$

Hence ϕ_P is simply the mean of the face values ϕ_w, ϕ_s and ϕ_d because $\mathbf{u}>0$ in each component direction. It should be noted that, if $\mathbf{u}<0$ in any one direction, then the CBC will require that $\phi_w=\phi_P$ instead of $\phi_e=\phi_P$ (in the x-direction, say). Hence there is no loss of generality by taking the components of $\mathbf{u}$ to be positive in all directions.

Now, since the CBC requires that $\phi_w\in[\phi_W, \phi_P]$, $\phi_s\in[\phi_S, \phi_P]$ and $\phi_d\in[\phi_D, \phi_P]$, ϕ_P cannot be greater (or less) than ϕ_W, ϕ_S and ϕ_D simultaneously. Therefore the computed ϕ_P given by an approximation which satisfies the CBC (in each co-ordinate direction) cannot lie outside the range of its nearest neighbours at the E, W, N, S, U and D nodes.

APPENDIX II: ADI–PENTADIAGONAL MATRIX ALGORITHM (PDMA)

The ADI–PDMA approach is advantageous for use with high-order approximations to the convective term because:

1. It has the combined advantage of simplicity and a low storage requirement.
2. The coefficient matrices **A** generated by schemes such as CCCT, QUICK and CUI require no special reformulations as would be the case if a TDMA were employed.
3. When an ADI solution procedure is adopted, the current line is solved exactly.

Making use of the notation employed in Appendix I then, if the y and z values (say) of the dependent variable along an x-direction (east–west) grid line are fixed at their previous iterative values, the set of quasi-linear algebraic equations thus generated can be written in the following form:

$$-A_{EE}\phi_{EE}-A_E\phi_E+A_P\phi_P-A_W\phi_W-A_{WW}\phi_{WW}=\mathscr{S}_P, \tag{24}$$

where $\mathscr{S}_P=\sum A_m\phi_m+S_P$ and $m=$ N, S, NN, SS, U, D, UU and DD.

Applying (24) at all nodal points k along this grid line results in a pentadiagonal coefficient matrix which can be decoupled by LU-decomposition to generate the following recursive procedure:

$$(\phi_P)_k=v_k-\delta_k(\phi_P)_{k+1}-\lambda_k(\phi_P)_{k+2}, \tag{25}$$

where

$$v_k=((\mathscr{S}_P)_k-\beta_k v_{k-1}-\sigma_k v_{k-2})/\gamma_k \tag{26}$$

and

$$\begin{aligned}
&\sigma_k=-(A_{EE})_k, && \beta_k=-(A_E)_k-\sigma_k\delta_{k-2},\\
&\gamma_k=(A_P)_k-\sigma_k\lambda_{k-2}-\beta_k\delta_{k-1}, && \delta_k=-[(A_W)_k+\beta_k\lambda_{k-1}]/\gamma_k,\\
&\lambda_k=-(A_{WW})_k/\gamma_k. &&
\end{aligned} \tag{27}$$

To obtain a solution throughout the computational domain of interest, the above procedure is followed on each of the east–west grid lines in turn, using the most recently calculated values from the previous grid line. The procedure is then repeated in the remaining co-ordinate directions (y and z). This pattern can be repeated any number of times to achieve a desired level of accuracy.

REFERENCES

1. P. J. Roache, *Computational Fluid Dynamics*, Hermosa, Albuquerque, 1976.
2. R. D. Richtmyer and K. W. Morton, *Difference Methods for Initial-Value Problems*, Interscience, New York, 1967.
3. B. P. Leonard, 'A stable and accurate convective modelling procedure based on quadratic upstream interpolation', *Comput. Methods Appl. Mech. Eng.*, **19**, 59–98 (1979).

4. B. P. Leonard, 'A survey of finite differences of opinion on numerical muddling of incomprehensible defective confusion equation', paper in *ASME, Applied Mechanics Division, Winter Annual Meeting*, 1979.
5. R. K. Agarwal, 'A third-order-accurate upwind scheme for Navier–Stokes solution at high Reynolds numbers', *Paper No. AIAA-81-0112, AIAA 19th Aerospace Science Meeting, St. Louis*, 1982.
6. B. P. Leonard, 'Adjusted quadratic upstream algorithms for transient incompressible convection', *AIAA- J.*, 226–233 (1979).
7. W. Shyy, 'A study of finite-difference approximation to steady-state, convection dominated flow problems', *J. Comput. Phys.*, **57**, 415–438 (1985).
8. P. H. Gaskell and A. K. C. Lau, 'An efficient solution strategy for use with high-order discretization schemes', *Report No. T40*, Department of Mechanical Engineering, University of Leeds, 1986.
9. G. D. Raithby, 'Skew upwind differencing for problem involving fluid flow', *Comput. Methods Appl. Mech. Eng.*, **9**, 153–164 (1976).
10. S. A. Syed, A. D. Gosman and M. Peric, 'Assessment of discretization schemes to reduce numerical diffusion in the calculation of complex flows', *Paper No. AIAA-85-0441, AIAA 23rd Aerospace Science Meeting, Reno*, January 1985.
11. P. H. Gaskell and A. K. C. Lau, 'An assessment of direct stress modelling for elliptic turbulent flows with the aid of a non-diffusive, boundedness preserving, discretization scheme', *Proc. 5th Int. Conf. on Numerical Methods in Laminar and Turbulent Flow, Montreal*, 1987.
12. P. H. Gaskell and N. G. Wright, 'Multigrids applied to an efficient fully coupled solution technique for recirculating fluid flow problems', *Proc. IMA Conf. on the Simulation and Optimisation of Large Systems, Reading*, 1986.
13. M. Atias, M. Wolfshtein and M. Israel, 'Efficiency of Navier–Stokes solvers', *AIAA J.*, **15**, 263–266 (1977).